Biochimica et Biophysica Acta 1848 (2015) 2868–2877

Contents lists available at ScienceDirect

Biochimica et Biophysica Acta

journal homepage: www.elsevier.com/locate/bbamem

Characterization of the cell penetrating properties of a human salivary proline-rich peptide

Giorgia Radicioni [a], Annarita Stringaro [b], Agnese Molinari [b], Giuseppina Nocca [a], Renato Longhi [c], Davide Pirolli [a], Emanuele Scarano [d], Federica Iavarone [a], Barbara Manconi [e], Tiziana Cabras [e], Irene Messana [e], Massimo Castagnola [a], Alberto Vitali [f,*]

[a] Istituto di Biochimica e Biochimica Clinica, Facoltà di Medicina, Catholic University, L.go F. Vito, 1, 00168 Rome, Italy
[b] Dipartimento di Tecnologie e Salute, Istituto Superiore di Sanità, Viale Regina Elena, 299, 00161 Rome, Italy
[c] Istituto per la Chimica del Riconoscimento Molecolare, Italian National Research Council, Via Mario Bianco, 9, 20100 Milan, Italy
[d] Dipartimento di Otorinolaringoiatria, Facoltà di Medicina, Catholic University, Largo A. Gemelli, 8, 00168 Rome, Italy
[e] Dipartimento di Scienze Applicate ai Biosistemi, University of Cagliari, Cittadella Universitaria, Monserrato, 09042 Cagliari, Italy
[f] Istituto per la Chimica del Riconoscimento Molecolare, Italian National Research Council, Rome, L. go F. Vito, 1, 00168 Rome, Italy

ARTICLE INFO

Article history:
Received 29 April 2015
Received in revised form 22 July 2015
Accepted 27 August 2015
Available online 29 August 2015

Keywords:
Proline-rich peptide
Saliva
Cell internalization
Flow cytometry
Laser scanning confocal microscopy

ABSTRACT

Saliva contains hundreds of small proline-rich peptides most of which derive from the post-translational and post-secretory processing of the acidic and basic salivary proline-rich proteins.
Among these peptides we found that a 20 residue proline-rich peptide (p1932), commonly present in human saliva and patented for its antiviral activity, was internalized within cells of the oral mucosa. The cell-penetrating properties of p1932 have been studied in a primary gingival fibroblast cell line and in a squamous cancer cell line, and compared to its retro-inverso form. We observed by mass-spectrometry, flow cytometry and confocal microscopy that both peptides were internalized in the two cell lines on a time scale of minutes, being the natural form more efficient than the retro-inverso one. The cytosolic localization was dependent on the cell type: both peptide forms were able to localize within nuclei of tumoral cells, but not in the nuclei of gingival fibroblasts. The uptake was shown to be dependent on the culture conditions used: peptide internalization was indeed effective in a complete medium than in a serum-free one allowing the hypothesis that the internalization could be dependent on the cell cycle. Both peptides were internalized likely by a lipid raft-mediated endocytosis mechanism as suggested by the reduced uptake in the presence of methyl-ß-cyclodextrin. These results suggest that the natural peptide may play a role within the cells of the oral mucosa after its secretion and subsequent internalization. Furthermore, lack of cytotoxicity of both peptide forms highlights their possible application as novel drug delivery agents.

1. Introduction

The proline-rich peptides are an interesting and heterogeneous group of molecules characterized by the presence of a high percentage of proline residues, feature that confer them peculiar structural and functional characteristics [1]. They are present not only in saliva, but also in diverse body cells, tissues and compartments such as skin [2], tears [3], colostrum [4] and neurohypophysis secretion granules [5]. They were firstly discovered to possess antimicrobial activities [6], further, they were recognized as modulator of transduction signals and inter-molecular interactions [7,8]. One of the characteristics of some proline-rich peptides is their ability to cross the cell membrane without a damage [9] and exploiting their activity intracellularly, interacting with molecular targets represented by specific protein modules [10,11]. Furthermore, in the cell penetrating peptide (CPP) panorama, the proline-rich peptides are considered promising tools for the drug delivery [12,13]. CPPs are widely studied for their ability to enter

Abbreviations: MALDI-TOF, Matrix Assisted Laser Desorption Ionization-Time of Flight; R.I., retro-inverso; PRPs, proline-rich proteins; CPP, cell penetrating peptide; FC, flow cytometry; LSCM, laser scanning confocal microscopy; TFA, trifluoroacetic acid; FAM, 5-carboxyfluorescein; hGFs, human gingival fibroblasts; FCS, fetal calf serum; HBSS, Hanks' balanced salt solution; IDMEM, Iscove's Modified Eagle Medium; DMEM, Dulbecco's Modified Eagle's Medium; NRU, neutral red uptake; MTT, thiazolyl blue tetrazolium bromide; DPBS, Dulbecco's Phosphate-Buffered Saline; RIPA, radio immunoprecipitation assay

* Corresponding author at: Istituto per la Chimica del Riconoscimento Molecolare, Italian National Research Council (CNR), Rome, L.go F. Vito, 1, 00168 Rome, Italy.
E-mail addresses: gradicioni@yahoo.it (G. Radicioni), annarita.stringaro@iss.it (A. Stringaro), agnese.molinari@iss.it (A. Molinari), g.nocca@rm.unicatt.it (G. Nocca), renato.longhi@icrm.cnr.it (R. Longhi), davide.pirolli@rm.unicatt.it (D. Pirolli), escarano@rm.unicatt.it (E. Scarano), federica.iavarone@rm.unicatt.it (F. Iavarone), bmanconi@unica.it (B. Manconi), tcabras@unica.it (T. Cabras), imessana@unica.it (I. Messana), massimo.castagnola@icrm.cnr.it (M. Castagnola), alberto.vitali@icrm.cnr.it (A. Vitali).

http://dx.doi.org/10.1016/j.bbamem.2015.08.019
0005-2736/

cells without disrupting or damaging the plasma membrane, and this feature is used for the design of cargoes for the delivery of bioactive molecules (e.g.: other peptides, RNA, DNA, antibodies) or drugs [14]. The small salivary proline-rich peptides mainly derive from the proteolytic cleavage process of the – acidic and basic– salivary proline-rich proteins (PRPs), which occur before granule storage and during and after granule secretion under the action of a complex set of endo- and exo-proteinases. The main cleavage site of PRPs is represented by the Gln-Gly site and as a consequence of this, hundreds of peptides showing highly similar and, often, overlapping sequences are generated. A great effort has been done to define the salivary peptidome [15], which is estimated to comprise more than 2000 peptides with an important qualitative contribution of other sources, such as the epithelial cells and the microbiome [16], being only 400–600 directly derived from salivary glands [17–19]. Despite these abundant structural data, no specific biological role has been assigned yet to anyone of these peptides. In this view the hypothesis that even some salivary proline-rich peptides may be internalized and exerting their function inside the cells of oral mucosa, is intriguing. The peptide p1932 (NH_2-GPPPQGGNKPQGPPPPGKPQ), is commonly found in human saliva [19] and its characteristics, such as the basic character and the small dimensions, are compatible with the ability to enter cells. In this study we have investigated different aspects of this peptide related to its cellular uptake in an oral squamous cancer cell line and in a primary gingival fibroblast cell line. The uptake rates and cytosolic distribution of p1932 peptide and of its retro-inverso counterpart (R.I.-p1932) have been also investigated and compared.

The results obtained let us to hypothesize that p1932 may be considered as a natural cell-penetrating peptide whose biological function may be exploited once inside the cells.

2. Materials and methods

2.1. Peptide synthesis and labeling

P1932, R.I.-p1932 peptides and penetratin were assembled on an Applied Biosystem Peptide Synthesizer 433A (Foster City, CA, USA) on a preloaded proline-2-chlorotrityl resin (Novabiochem, Laufelfingen, CH) following the Fmoc-(N^{α}-9-fluorenylmethyloxycarbonyl) protocol for stepwise solid phase peptide synthesis [20]. Fmoc-amino acids were from Novabiochem. All couplings were carried out with 5 fold excess of activated amino acid in the presence of 10 equivalents of *N*-ethyldiisopropyl amine, using *N*-[(dimethylamino)-1-*H*-1,2,3-triazole-[4,5-β] pyridine-1-ylmethylene]-*N*-methylmethanaminium hexafluorophosphate *N*-oxide (HATU, PE Biosystems, Inc., Warrington, UK) as activating agent for the carboxy group. The fluoresceinated peptides were obtained by extending the N-termini of an aliquot (15%) of the assembled peptide-resin with 8-(9-fluorenyloxycarbonyl-amino)-3,6-dioxaoctanoic acid, removal of the Fmoc protecting group and coupling of FAM, mediated with 1-hydroxybenzotriazole and *N*, *N*′-diisopropylcarbodiimide. The fluoresceinated peptide was released from the resin and purified by the same procedures adopted for the free-peptide. At the end of peptide chain assembly, the peptide was cleaved from the resin by treatment with a mixture of 80% trifluoroacetic acid, 5% water, 5% phenol, 5% thioanisole, 2.5% ethanedithiol and 2.5% triisopropylsilane for 3 h, with concomitant side chain deprotection. After filtration of the resin the peptide was precipitated in cold *tert*-butylmethyl ether. After centrifugation and washing with *tert*-butylmethyl ether the peptide was suspended in 5% aqueous acetic acid and lyophilized. Analytical and semipreparative Reversed Phase High Performance Liquid Chromatography (RP-HPLC) was carried out on a Tri Rotor-VI HPLC system equipped with a MD-910 multichannel detector for analytical purposes or with a Uvidec-100-VI variable UV detector for preparative purpose (all from JASCO, Tokyo, Japan). Analytical RP-HPLC was performed on a Jupiter 5 μm C18 300 Å column (150 × 4.6 mm, Phenomenex, Torrance CA, USA). Semipreparative RP-HPLC was performed on a Jupiter 10 μm C18 300 Å (250 × 21.2 mm, Phenomenex, Torrance CA, USA). Linear gradients of acetonitrile in aqueous 0.1% TFA (v/v) were used to elute bound peptide. MALDI-TOF mass spectrometry analyses performed on an Autoflex workstation (Bruker Daltonics, Bremen, DE) confirmed the theoretical mass of the peptide.

2.2. Cell cultures

Unless otherwise specified, all chemicals and reagents used in this section were obtained from Sigma (Milan, Italy). PE/CA-PJ15 cells (ECACC, Porton Down, UK) were cultured at 37 °C in a humidified environment (5% CO_2) in IDMEM supplemented with 10% FCS, 500 units/mL penicillin, 10 mg/mL streptomycin, 20 mM L-glutamine. HGFs were obtained (with informed consent) from a healthy patient subjected to gingivectomy of the molar region. Immediately after removal the tissues were placed in HBSS solution with penicillin (250 U/mL), streptomycin (0.25 mg/mL), gentamycin (0.05 mg/mL), and amphotericin B (0.0025 mg/mL). The epithelial layer was detached mechanically and the sub-epithelial specimens were plated in tissue culture flasks with DMEM, supplemented with 50% FCS, L-glutamine (2 mM), sodium pyruvate (1 mM), penicillin (50 UI/mL) and streptomycin (50 μg/mL), at 37 °C in a 5% humidified CO_2 atmosphere. After the first passage, the hGFs were routinely cultured in DMEM supplemented with 10% FCS [21–23] and were not used beyond the fifth passage [24]. Cell synchronization was performed culturing the cells in a serum free medium for 24 h.

2.3. Cytotoxicity and membrane perturbation assays

Cytotoxic of p1932 and R.I.-p1932 was evaluated on PE/CA PJ15 and hGF cell lines by means of MTS (Promega, Madison, WI, USA) and NRU tests. Lyophilized peptides were dissolved in basal medium checking for the final pH. Cells (1×10^4) suspended in 200 μL of basal medium, were seeded in individual wells of a 96-well microplate and cultured to subconfluent monolayer for 24 h. Cell viability was evaluated at 24 h, 48 h, and 72 h after the addition of increasing concentrations (2.5, 5, 10, 20, 50 and 100 μM) of the peptides at 37 °C. NRU assay was performed according to [25] reading the absorbance at 540 nm. MTS assay was performed accordingly to manufacture protocols. Absorbance values were measured using an automatic microplate photometer (Packard Spectracount™, Packard BioScience Company, Meriden, CT, USA). Each experiment was performed in sextuplicate.

Dimyristoyl-phosphatidyl glycerol (DMPG), phosphatidylcholine (PC) and 10,12-Tricosadiynoic acid (polydiacetylene PDA) and melittin, were all purchased from Sigma-Aldrich. Melittin was used as a positive control. Phospholipid vesicles were prepared as described [9,26]. The resulting vesicles exhibited an intense blue color. The experiments were performed with a spectrophotometer (Agilent 8453, Santa Clara, CA) following the signals at 500 and 640 nm in the time. In order to quantitatively evaluate the colorimetric response the extent of blue-to-red color transition was calculated by the colorimetric response (%CR), which is defined as:

$$\%CR = [(PB_0 - PB_I)/PB_0] \times 100 \quad (1)$$

where $PB = A_{640} / (A_{640} + A_{500})$, A is the absorbance either at 640 nm (blue color) or at 500 nm (red component) in the UV–vis spectrum, PB_0 is the red/blue ratio of the control sample (before induction of color change), and PB_I is the value obtained after the addition of peptides to the vesicle solutions.

2.4. MALDI-TOF analysis of internalization

Cells were seeded into 6-well culture plates (Falcon, BD Bioscience, Milan, Italy) and held for 48 h in a medium supplied with serum. 200 μL of a 100 μM peptide solution was applied for 30 min at 37 °C, 5% CO_2 (final concentration of the peptide 20 μM). After rinsing with

PBS, cells were treated for 10 min at 37 °C with 200 mL of a trypsin solution (0.05% trypsin, 0.02% EDTA w/v) and pronase before lysis, then washed twice with PBS, and centrifuged at 4000 rpm for 10 min at 4 °C. Cell pellets were suspended in 200 μL of lysis buffer (Tris 10 mM, EDTA 1 mM, pH 7.5) added of Protease Inhibitor Cocktail (Sigma), incubated for 1 h at 4 °C and then sonicated for 15 min. Finally, samples were centrifuged at 9000 rpm for 5 min at 4 °C. To remove contaminating salts and to concentrate, samples were cleaned with C-18 Zip-Tips (Millipore, Billerica, MA, USA) and 1 μL of the resulting solution was mixed (1:1 v/v) with 0.3% α-hydroxy-cinnamic acid and spotted on a stainless MALDI-TOF target until dryness. Spectra were collected in a positive linear mode with a laser frequency of 5 Hz. At least 300 scans have been integrated to optimize the signal/noise ratio.

2.5. Flow cytometry

Exponentially growing cells were dissociated with trypsin, and 5×10^5 cells were plated and cultured overnight on 30 mm plates. The culture medium was discarded and cells were washed twice with PBS. The cell monolayer was incubated with peptides (20 μM final concentration) dissolved in FCS free medium for the appropriate exposure time (5, 15, 30 min). After incubation cells were rinsed twice with PBS and then dissociated with trypsin. Cell suspension was centrifuged at 1500 rpm for 5 min. The cell pellet was washed twice with DPBS and then suspended in 250 μL of PBS. Samples were then analyzed on the FACScan flow cytometer. For the synchronized cells the protocol was the same but cells were cultured in FCS free medium. The fluorescence emission was collected through a 670 nm band-pass filter and acquired in "log" mode. At least 10.000 events were analyzed. The fluorescence content was evaluated as fluorescence intensity, expressed as mean fluorescence channel (MFC). The analysis was performed by the CellQuest TM software (BD Bioscience, Milan, Italy). Values are reported as mean values obtained from 3 independent experiments. For the synchronized cell the protocol was the same but cells were cultured for 24 h in a FCS free medium.

2.6. Laser scanning confocal microscopy

To investigate the intracellular distribution of p1932 and R.I.-p1932 in the different cell lines, PJ15 and gingival fibroblast cells were analyzed by LSCM. Observations were performed by using a Leica TCS SP2 laser scanning confocal microscope (Leica Microsystems, Mannheim, Germany). Exponentially growing cells were dissociated with trypsin, and 7×10^4 cells were plated and cultured overnight in μ-Slide 8 well (Ibidi, Planegg, Germany). The culture medium was discarded and cells were washed twice with DPBS. The cell monolayer was incubated with peptides (10 μM) dissolved in FCS free medium for the appropriate exposure time. After incubation cells were rinsed twice with DPBS and left in DPBS added with 10% glucose for the observation of the living cells. External peptide fluorescence was quenched with a trypan blue solution [27]. As a negative control, non-treated cells and cells incubated with 5-carboxyfluorescein (FAM) alone were also analyzed. Labeled p1932 and R.I.-p1932 fluorescence was excited at 488 nm and collected in a 500–535 nm emission window. Fluorescence emissions were collected after passage through a DD488/543 filter. Images were processed by using LCS software (Leica Microsystems).

2.7. Uptake inhibition experiments

All inhibitors were obtained from Sigma, and the following inhibitor concentrations were employed: 30 μM chlorpromazine hydrochloride, 2.5 mM methyl-β-cyclodextrin, 10 μM heparin sodium salt all dissolved in Millipore water H_2O, while 10 μM cytochalasin-D was dissolved in DMSO at a concentration of 5 mg/mL and subsequently diluted in MilliQ water in order to obtain a final operative concentration of DMSO of 0.1%. Cells (5×10^3) were seeded in a 96 well microplate and incubated with inhibitors for 30 min in a serum-free medium; thereafter, proline-rich peptides were added (final peptide concentration 10 μM) and cells further incubated for 30 min. Excess of peptides and inhibitors was removed by rinsing twice with DPBS and external fluorescence was quenched by treating the cells for 1 min with trypan blue and subsequent washing. Finally, cells were treated with proteases (trypsin and pronase) and lysed with RIPA buffer. The resulting lysates were centrifuged at 12,000 rpm × 15 min to remove cell debris and the supernatants were collected and read in a Glomax (Promega, Madison, WI, USA) multiwell reader device using a fluorescence module with a 570 nm filter. Experiments of uptake at 4 °C were performed and followed by FC. Cells were left to equilibrate at this temperature for 15 min after while the peptides (20 μM final concentrations) were incubated and the internalization was followed in for 30 min (checks at 0, 15 and 30 min). Then, cells were placed at 37 °C and FC analyses were performed again at 0, 15 and 30 min. The data are the results of triplicate experiments.

2.8. Statistical analysis

Data are shown as mean ± standard deviation. Statistical significances were analyzed by ANOVA with a significance of <0.05 for P values. A Dunnett's test ($P < 0.05$) was performed on the full data set to compare values of control experiments with all other groups.

3. Results

3.1. p1932 and R.I.-p1932 are internalized within cells

In order to qualitatively evaluate the internalization of p1932 and its retro-inverso analogous, a MALDI-TOF mass spectrometry method has been employed. PE/CA PJ15 an oral squamous cancer cell line and primary human gingival fibroblasts (hGFs) were incubated in the presence of either p1932 or R.I.-p1932 peptides for 30 min; the mass spectra analysis of the cell lysates revealed that both the peptides were internalized after this time period (Fig. 1).

To quantitatively determine in a scale time the uptake of the two peptides, flow cytometry (FC) measurements were carried out. The extent of internalization was determined from the ratio between the intensity of fluorescence measured after peptide exposure and the control experiments. The FC measurements, even though slightly overestimated due to residual membrane-bound peptide fraction, revealed that the entry of the two peptide forms began already after 5 min upon incubation (Fig. 2A and B), an effect more evident in not synchronized cells.

In the following 30 min, a continuous linear increase of the fluorescence was observed indicating a constant entry of the peptides. The increase of fluorescence of p1932 peptide was faster in the PJ15 cell line than in hGFs, at least within the first 15 min, but the amount of peptide internalized after 30 min was comparable in both cell types (Fig. 2A). Internalization of the retro-inverso form resulted to be slower than p1932 in the same time of observation (Fig. 2B) in both cell types.

In order to confirm the above results and to observe the intracellular distribution of p1932 and of its R.I. form, we used laser scanning confocal microscopy (LSCM), and we operated on living cells in order to avoid artifacts due to the fixation [28]. The images (optical sections) were taken after 30 min and 1 h upon 10 μM peptide treatment and after quenching extracellular fluorescence with a trypan blue solution in order to avoid a green background due to the peptide excess (Fig. 3).

The green signal represents carboxyfluorescein-p1932 (FAM-p1932) or FAM-R.I.-p1932 (excitation 488 nm, emission 500–535 nm). LSCM observations of hGFs showed that p1932 was present after 30 min in diffuse punctuate structures (vesicles) distributed in a perinuclear pattern; after 60 min the fluorescence was more homogeneous, but nuclei still appeared almost completely negative for fluorescence (Fig. 3, panels 1 and 2). In PE/CA PJ15 cells after 30 min, many punctuate structures

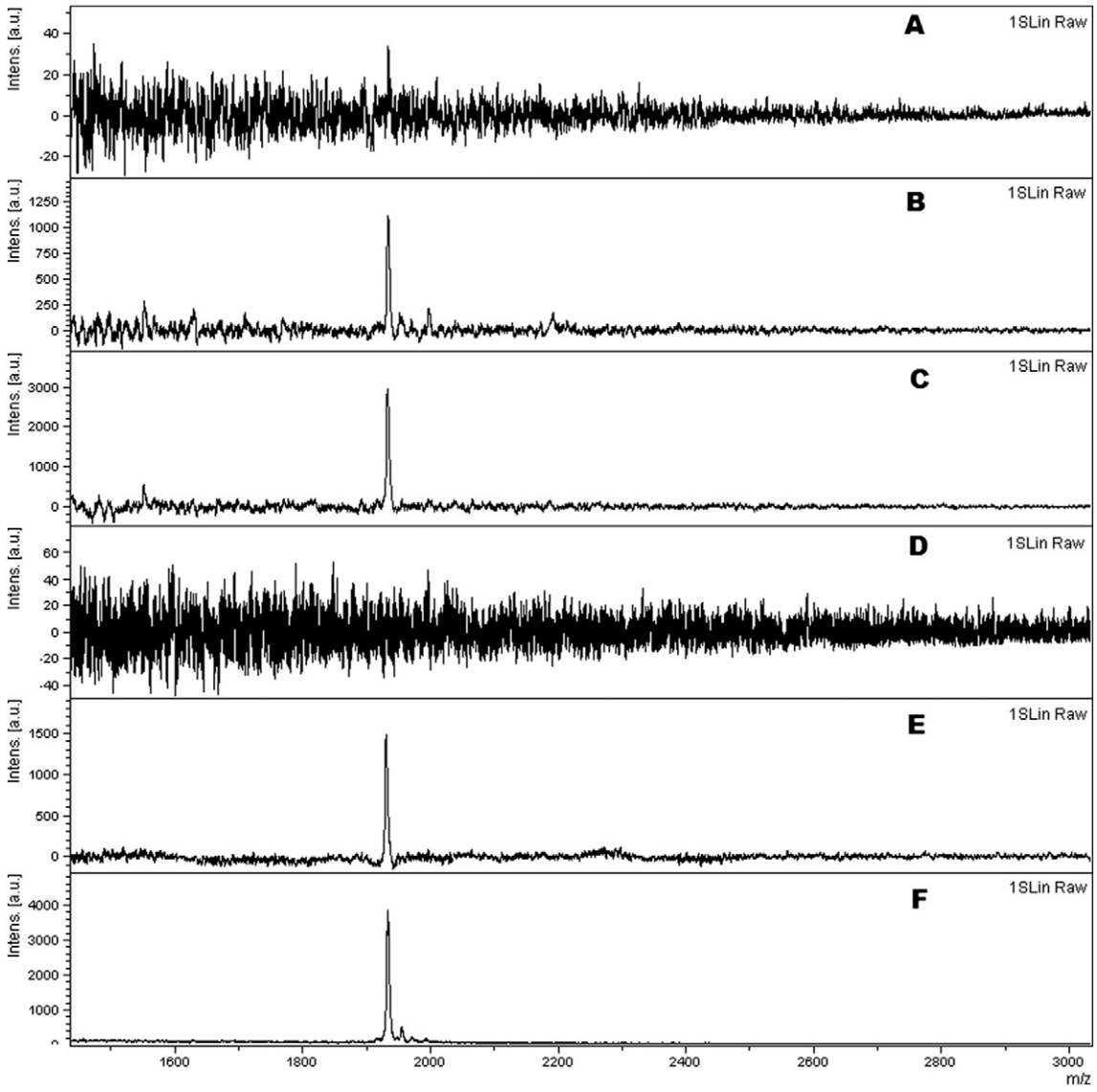

Fig. 1. MALDI-TOF-MS analysis of cells treated with p1932 and R.I.-p1932. MALDI-TOF-MS spectra of cell lysates were taken after 30 min upon treatment with 20 μM (final concentration) of each peptide. Each sample, after lysis, was concentrated and purified with Zip-Tip C18 and mixed with an HCCA matrix solution. Panel A: PE/CA PJ15 cells, control; Panel B: PE/CA PJ15 cells treated with p1932; Panel C: PE/CA PJ15 cells treated with R.I.-p1932. Panel D: hGF cells, control; Panel E: hGF cells treated with p1932; Panel F: hGF cells treated with R.I.-p1932.

are visible similar to hGFs, but is already evident a more diffusion into cytoplasmic organelles and nuclei, where after 60 min, p1932 was highly visible (Fig. 3, panels 5 and 6).

In a similar fashion to p1932, the retro-inverso form did not enter hGF nuclei (Fig. 2, panels 3 and 4), while it entered nuclei of PJ15 even if in a lesser extent if compared to p1932 (Fig. 2, panels 7 and 8). An endocytic uptake is suggested also for R.I.-p1932 due to the presence of many vesicles visible in both the cell lines.

A comparison with penetratin, a well-known cell-penetrating peptide employed in several studies as a cargo for the delivery of biological active molecules [29–31] was also carried out. As a result, penetratin showed a punctuate distribution nearby the plasma membrane and in the cytosol both in PJ15 cells and in hGFs (Fig. 3, panels 9–12). At 60 min a more diffuse distribution could be appreciated in hGFs differently from the punctuate patterns observed in PJ15.

3.2. The medium composition affects peptide uptake

Interesting results were observed comparing the effects of using a complete medium and a serum free medium. The two proline-rich peptide forms were separately incubated with PJ15 cells and hGFs previously maintained in a serum-free medium for 24 h, in this way, the cells have been blocked in their cell cycle. As a result, in the serum free condition the internalization process was dramatically reduced in both the cell lines and with both the peptide forms (Fig. 2A and B). More precisely, after 30 min the amount of p1932 within the cells was reduced by 80% in hGFs and by 75% in PJ15 cells (Fig. 2A and B), while R.I.-p1932 amount was lowered almost of the 60% in hGFs and 80% in PJ15 cells (Fig. 2A and B). For the calculation of the internalization rate, the amount of death cells due to serum-free medium treatment was taken in account.

3.3. Effect of endocytosis inhibitors on peptide internalization

To shed more light on the internalization processes involving p1932 and R.I.-p1932, we performed a series of uptake experiments at different temperatures and in the presence of specific inhibitors of various endocytosis pathways. The effect of temperature on peptide uptake was investigated performing experiments at 4 °C for 30 min and followed by means of FC. As a result, the internalization rates of p1932 and R.I.-p1932 were lowered by at least 70% in both cell lines, if compared to the rates measured at 37 °C (Fig. 4, inset).

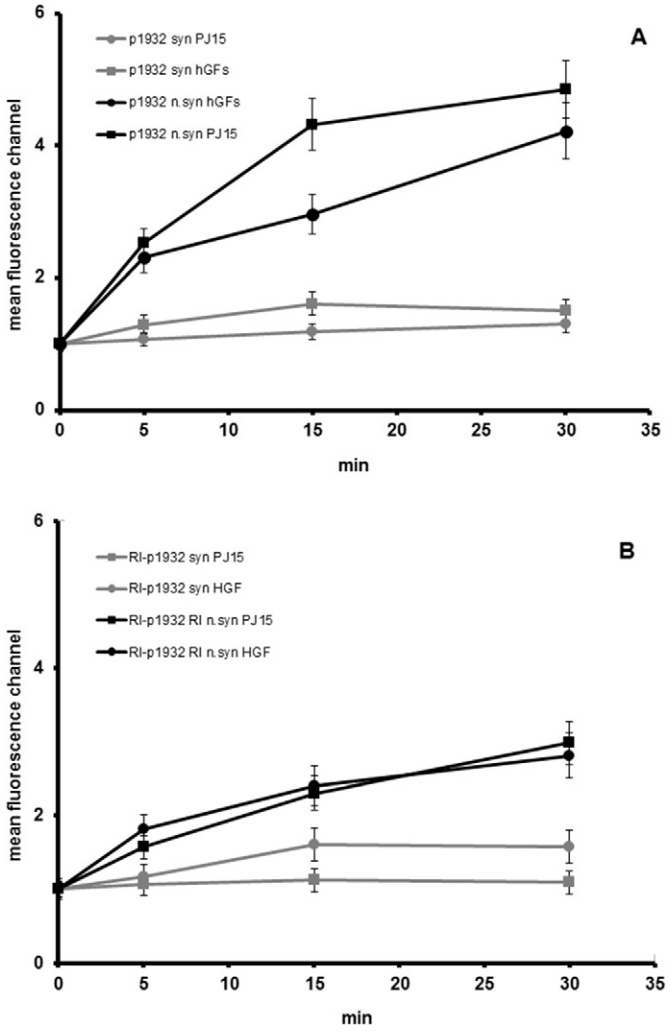

Fig. 2. Penetration rates of p1932 (A) and R.I.-p1932 (B) measured by FC. The fluorescence emission was collected through a 670 nm band-pass filter and acquired in "log" mode. Black lines represent the internalization rate in cells grown in a complete medium (not synchronized cells), while gray lines are representative of cells grown for 24 h in a serum-free medium (synchronized cells) at 37 °C, 5% CO_2 atmosphere. Peptides were used at 20 μM concentration. As a negative control, non-treated cells were also analyzed.

When "cooled" cells were placed at 37 °C, an increase in the internalization rates, more evident for p1932, could be observed in the following minutes. The different kinetic profiles registered with respect to the experiments shown in Fig. 2 may be likely due to the "in course" restoring to the standard temperature of the cells system (Fig. 4).

To demonstrate that an energy dependent endocytosis mechanism was at the basis of the two proline-rich peptide internalization, we used specific inhibitors of different uptake mechanisms: chlorpromazine for clathrin-mediated endocytosis, cytochalasin-D (Cyt-D) for macropinocytosis, methyl-β-cyclodextrin (M-β-CD) for lipid raft-caveolae endocytosis and heparin for heparansulfate dependent uptake. The results showed that in all the experiments the inhibitors behaved in a similar way independently from the cell type and from the peptide form, in particular chlorpromazine and Cyt-D did not affect peptides uptake while M-β-CD significantly inhibited the entry of the proline-rich peptides both in PJ15 and hGF cells (Figs. 5a, b, c and d).

Heparin had a lower, but significant effect on peptide internalization and to shed light on this last point, we examined if an interaction between heparin and p1932 and R.I.-p1932 occurred by using a size exclusion chromatography approach. The two peptides were mixed with increasing heparin amounts in order to have the following peptide: heparin ratios: 1:1, 1:2, 1:5 and 1:8. As a result, in the conditions used (PBS saline buffer, pH 7.4) a very poor modification in the elution volumes of peptides was seen (Table 1) indicating an absent or, at least, a weak interaction.

3.4. Cytotoxicity and artificial vesicle interaction studies

Cytotoxicity of p1932 and R.I.-p1932 was proven by MTS and the NRU assays against the PJ15 and hGF cell lines in the concentration range 2.5–100 μM. In any of these conditions, a substantial cytotoxicity could not be appreciated. Interestingly even the retro-inverso form showed a slight cytotoxicity at the concentration of 100 μM at which 85% and 82% of viability were measured for hGF and PJ15 cells, respectively.

The absent or low of cytotoxicity of p1932 and R.I. was also confirmed by the optical microscopy images where any evident morphological changes could be detected in both the cell lines after 60 min upon incubation with the peptides (Fig. 3, panels 13–16).

In order to confirm the microscopy data about concerning the absence of membrane perturbation and hence of a consequent cytotoxicity, we performed a lipid vesicle perturbation assay based on a colorimetric method developed by Kolusheva and coll. [26] in which suitable phospholipids and polydiacetylene (PDA) are mixed to give a UV-light sensible vesicles. The intact vesicles once activated by UV-light show a blue coloration that turns pink or red if a perturbation event occurs as in the case of the presence of a pore-forming peptide. As a result p1932 and R.I.-p1932 did not show any perturbation effect on artificial lipid–PDA vesicles when compared with melittin (Fig. 6), an antimicrobial peptide known to kill bacterial cells by a membrane disruptive pore-forming mechanism of action.

Accordingly with these data a sequence-based analysis of the hydropathy of the p1932 peptide with the freely available MPEx web tool (http://blanco.biomol.uci.edu/mpex/) was performed. MPEx allows to explore the topology of membrane proteins by means of hydropathy plots based upon thermodynamic and biological principles, as well as to calculate the theoretical free energy related to the transfer of a peptide from water to a POPC interface (or vice versa). The transfer free energy derives from the sum of the free energy contributions calculated on the basis of the Wimley–White scale [32]. The water–lipid bilayer transfer free energy value was found to be + 8.24 kcal/mol for p1932, suggesting a poor ability of the peptide itself to pass through the biological membrane by passive diffusion.

3.5. Circular dichroism studies

P1932 and its retro-inverso form were analyzed by FAR-UV circular dichroism in a phosphate buffer (25 mM, pH 7.0) at 25 °C and in a 2,2,2-trifluoroethanol (TFE)/phosphate buffer (30%, v/v) solution to mimic the membrane environment (Fig. 7).

In phosphate buffer the two peptides showed mirror images with a curve profile typical of an unordered structure characterized by a negative (for p1932) and a positive (for R.I.-p1932) band at 200 nm. In TFE 30% the spectrum of R.I.-p1932 remained the same, while a slight change in the conformation of p1932 could be observed represented by a slight positive increase at 219 nm showing a more susceptibility of the natural form to the solvent system used and a more structural flexibility. Interestingly, the positive increase at 219 nm may indicate an intrinsic propensity of p1932 to adopt a polyproline-II helix structural arrangement.

4. Discussion

The biological role of many salivary peptides is not completely understood; histatins play important roles in tissue repair events [33], and are involved in oral defense against pathogens [34] together with cathelicidin LL-37 and defensins [35]. Statherin together with other proline-rich proteins is implied in the enamel pellicle formation by

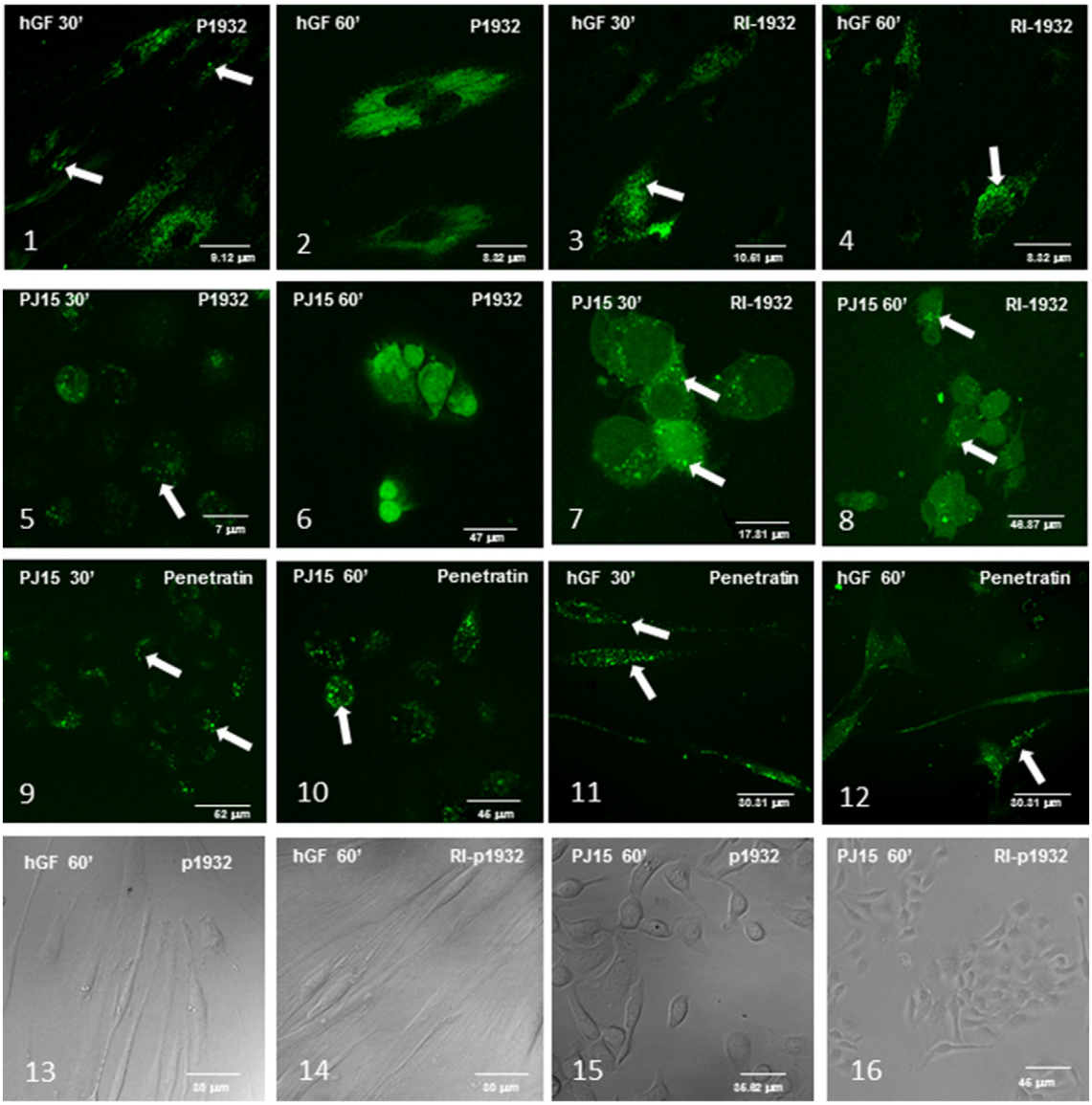

Fig. 3. Intracellular localization of p1932 and R.I-p1932 in PE/CA-PJ15 and hGF cells analyzed by laser scanning confocal microscopy. Concentration of peptides was 10 μM. The images were taken at 30′ and 60′ in order to observe the variable diffusion in the cells. Green signals: FAM-peptide's fluorescence (excitation 488 nm, emission 500–535 nm). From top left to bottom right: human gingival fibroblasts treated with p1932 (panels 1–2) and with R.I-p1932 (panels 3–4). PE/CA PJ15 cells treated with p1932 (panels 5–6) and with R.I.-p1932 (panels 7–8). Panels 9–12: experiments performed with FAM-penetratin with PJ15 (9–10) and hGFs (11–12). The arrows indicate the cytosolic vesicles containing the peptides. Bottom images (13–16): light images of hGF and PJ15 cells treated with proline-rich peptides taken at 60 min upon incubation. Representative images from three independent experiments are shown.

binding calcium and hydroxyapatite [36], and proline-rich proteins, such as IB-5 characterized by the repetitive sequence -KPQGPPPP-, seem involved in dietary tannin binding [37]. Hundreds of small-medium sized proline-rich peptides showing highly overlapping frames and similar sequences are generated by the pre-and post-secretory events occurring at the expenses of the salivary basic proline-rich proteins [15–17], but their function is almost still unknown. Among these, a 20 residues peptide (p1932, NH_2-GPPPQGGNKPQGPPPPGKPQ) was already patented by some of authors of this study for its strong anti-viral activity [PCT/IB2012/050415].

In consideration of the recognized cell penetrating properties of other analogy with other amphipathic proline-rich peptides [12], the present study was focused on the internalization properties of p1932. We focused on its internalization properties using two oral cell lines: a primary gingival fibroblast cell line produced in our laboratories and the PE/CA PJ15 cell line originated from an oral squamous cell carcinoma (OSCC) representative of an aggressive head and neck cancer [38]. p1932 peptide is commonly found in human saliva, deriving from the proteolytic processing of the proline-rich proteins PRB1-L (UniProt/Swiss-Prot P4280), PRB-2L (P02812/Q7M4Q5), PRB1-M (Q86YA1) [19]. The sequence of p1932 is repeated four times in PRP1-L and PRB-2L, and three times in PRB1-M, bringing its average concentration in human saliva to 5–10 μM depending on different factors (day time of collection, sex and age). Interestingly it is also found in G7N674 from *Macaca mulatta* and in G3RMU1 and G3RWV9 in *Gorilla gorilla*.

In this study we wanted to study also the retro-D version (R.I.) of the natural peptide in order to have a structural and a functional comparison. The internalization of the p1932 and R.I.-p1932 proline-rich peptides was initially followed by means of a MALDI-TOF mass spectrometry approach [39] as it is a quite simple, rapid and sensible method, and where peptides had necessarily not to be labeled, and thus preserving their natural structure and physicochemical properties. From a qualitative point of view the mass analysis showed that the natural peptide and its retro-inverso form were internalized within the first 30 min upon incubation, a reasonable time for consider them as cell-

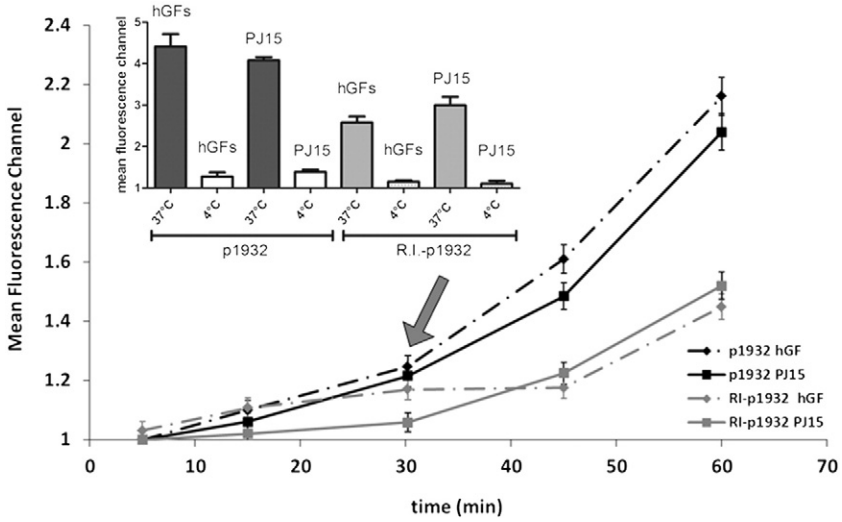

Fig. 4. Effect of temperature on peptide uptake. The line graph shows the uptake rates analyzed in the time by FC. HGF (black diamonds) and PE/CA PJ15 cells (black squares) treated with p1932. HGF (gray diamonds) and PJ15 cells (gray squares) treated with R.I.-p1932. Experiments were carried out at 4 °C at 5%, CO_2 atmosphere using a 20 μM peptide final concentration. The arrow indicates the return to 37 °C condition. To better appreciate the effect of temperature, the inset shows the effect of an exposure for 30 min at 4 °C on peptide uptake.

penetrating peptides. A more accurate time-based analysis was performed by means of FC where, even considering a slight overestimation of the cell surface-bound peptide. It was observed that p1932 was rapidly internalized by hGFs and tumoral cells within the first 15 min upon incubation, while the R.I. form resulted to be slower, a trend observed also in LSCM images where in the same time lapse, the cytosolic diffusion of the peptides appeared differently expressed. This aspect arises the question if the different peptide configuration may influence their uptake. Until a few years ago, the paradigm -chirality has no effect on CPPs uptake- was a rule, but recently this was demonstrated to be not completely true. In agreement with what observed for p1932 and R.I.-p1932, it was recently demonstrated that L- and D-polyarginine peptides may actually show a diverse uptake efficiency which was dependent both on their chirality and on the cell type employed [40]. As reported for the polyarginine peptides [40], L- and retro-D-p1932 may unspecifically bind heparan-sulfate on the plasma membrane and then be internalized by a chirality dependent uptake mechanism. Furthermore, the CD spectra profiles of p1932 and R.I.-p1932 taken in a phosphate buffer, show roughly mirror images, as they evidently share in this solvent similar secondary structure elements resembling a random coil arrangement. Nevertheless, in a more hydrophobic environment due to the addition of TFE p1932 showed to be more flexible

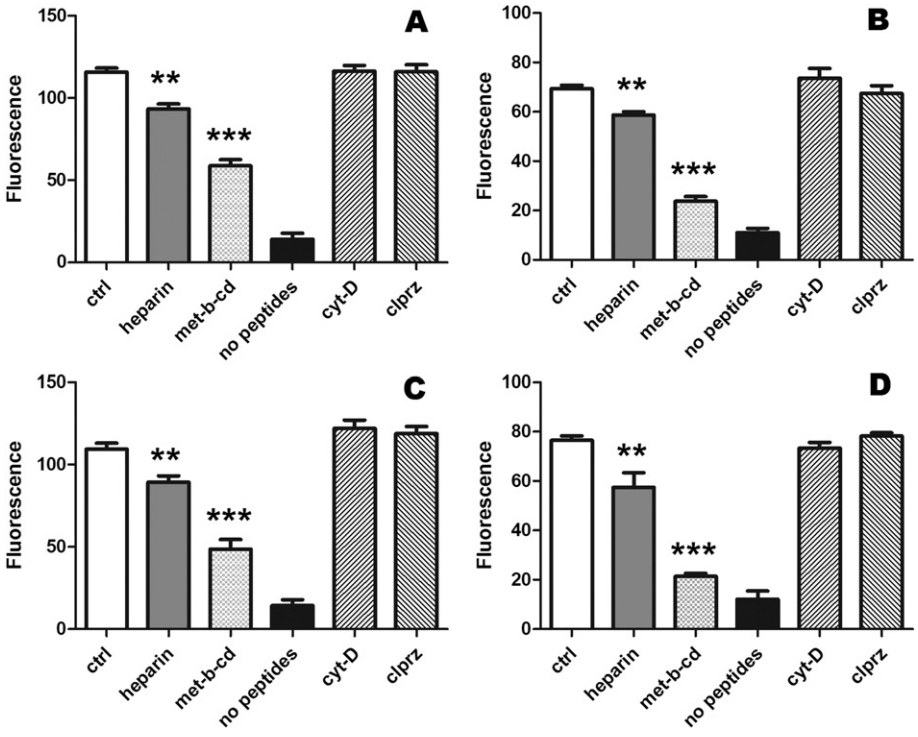

Fig. 5. Effect of uptake inhibitors. The scheme represents the effect of specific inhibitors on uptake mechanisms: heparin for GAGs mediated uptake mechanisms, methyl-β-cyclodextrin (met-b-CD) for lipid-raft/caveolae mediated endocytosis, chlorpromazine (clprz) for clathrin mediated endocytosis and cytochalasin-D (Cyt-D) for macropinocytosis. Schemes A) and B) PJ15 cells treated with p1932 and R.I-p1932 respectively. Schemes C) and D) hGFs treated with p1932 and R.I.-p1932 respectively. The fluorescence values were taken after lysis of the cells and readings. Peptides were used at a 10 μM concentration throughout. Control (CTRL) experiments were carried out with peptides without inhibitors. The "no peptides" columns are representative of the signal emitted by cells alone. Asterisks are representative of the statistical significance (** = good, *** = high, $P < 0.05$).

Table 1
The table shows the elution volumes obtained upon size exclusion chromatography runs of different mixtures of proline-rich peptides and heparin. The peptides were maintained at a fixed concentration of 1 mM while the amount of heparin was increased as reported.

	Control	1:1	1:2	1:5	1:8
p1932	18	18	18	17.5	17.2
R.I.-p1932	19	19	19	18.7	18.3

than R.I.-p1932. A retro-inverso peptide (a.k.a. retro-all-D- or retro-enantio-peptide) is made up of D-amino acids in a reversed sequence assuming a side chain topology similar to that of its natural counterpart, but with inverted amide peptide bonds. This feature may indeed affect the peptide structural flexibility as reported for other peptides [41–43]. Thus, the slower rate of cellular uptake of R.I.-p1932 may also be due to an affected interaction with the cell membrane apparatus determined by the structural arrangement of this peptide, an aspect, which has been considered important for the internalization of CPPs [44].

It appeared that the different stereochemistry of the peptides also influenced their cytosolic distribution, at least in PJ15 cancer cells. The confocal microscopy images shown that p1932 and more evidently its isomer, were internalized in vesicles (punctuate structures in the LSCM images) thus suggesting an endocytic pathway followed by both the peptides. In the same time lapse (60 min) while p1932 diffuse more rapidly in the cytosol of PJ15, also occupying the nuclei, the R.I.-p1932 was still present in vesicles and only partially diffused in the cytosol and nuclei of PJ15 that consequently showed a less intense fluorescence (Fig. 2). Completely different was the behavior in hGFs, where both the peptides were internalized by vesicles as demonstrated by the several punctuate structures in confocal images, and both were excluded from the nuclei even after 60 min upon exposure.

Thus, to confirm an endocytic pathway for p1932 and R.I.-p1932 uptake, as suggested by LSCM images, we performed experiments at 4 °C and subsequently with selected endocytosis inhibitors. Firstly, we tried to distinguish if a simple diffusion could be at the basis of proline-rich peptide uptake, in fact, energy dependent cell mechanisms such as endocytosis are strongly depleted at 4 °C [45], while diffusion or translocation is affected in a lesser extent or at all. The reduction of proline-rich peptide uptake compared to the rates observed at 37 °C (Fig. 4) strongly confirmed that an energy dependent mechanism was the main responsible for the peptide uptake also in agreement with the transfer free energy value obtained by MPEx web tool, indicating a low propensity of this peptide to translocate a lipid bilayer for passive diffusion.

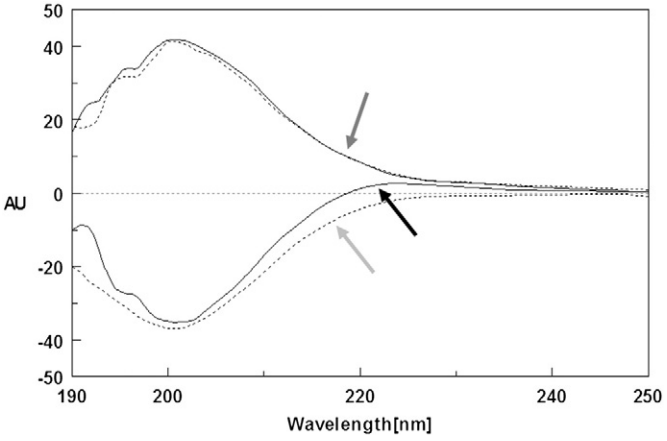

Fig. 7. Far-UV circular dichroism spectra of p1932 (light gray and black arrows) and R.I.-p1932 (dark gray arrow) at 25 °C. The peptides (all at 1 mM of concentration) were suspended in a 25 mM phosphate buffer, pH 7.0 (dotted lines) and in 30% 2,2,2-trifluoroethanol (continuous lines).

The internalization process is a very complex event and as outlined above, may be merely divided into two fundamental steps. The first one is the electrostatic interaction between the cationic moieties of a peptide (arginine and lysine) and the negative charges due to the polysulfated cell-surface glycosaminoglycan (GAG) polysaccharides [46,47]. The second step is the definitive entry, which can occur via different kinds of endocytosis pathways such as macropinocytosis, clathrin-dependent endocytosis (CDE) and lipid-raft/caveolae endocytosis. Chlorpromazine, cytochalasin-D, methyl-β-cyclodextrin (M-β-CD) and heparin are respectively usually employed as inhibitors of CDE, macropinocytosis, lipid-raft/caveolae endocytosis and binding to cell-surface GAGs mediated endocytosis [48]. Among these, M-β-CD had a clear inhibition effect on proline-rich peptide uptake, suggesting that a lipid raft mediated mechanism was the main way followed by these peptides for their internalization, in fact, M-β-CD acts as a cholesterol-sequestering agent and selectively inhibits the lipid raft formation that are definite regions of the plasma membranes particularly enriched of sphingolipids and cholesterol [49]. Accordingly to our data, a lipid raft based mechanism was demonstrated for the entry in He-La cells of the “sweet arrow” CF-(VRLPPP)3, an amphipathic

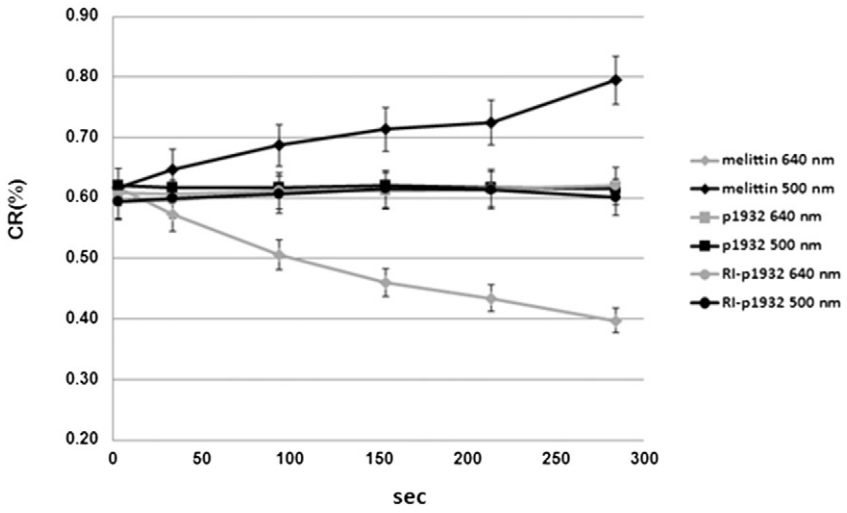

Fig. 6. Colorimetric phospholipid vesicle assay. Colorimetric response (%CR) induced by 20 μM p1932, R.I.-p1932 and melittin (positive control) on PC/DMPG/PDA vesicles at pH 7.4 was determined. % CR represents the percentage of color transition from blue (integral vesicles) to pink-red (perturbed vesicles) monitored at 640 nm and 500 nm, respectively.

proline-rich peptide [50]. From an applicative point of view, an uptake based on lipid rafts, differently from a clathrin-dependent endocytosis, is particularly attractive because the CPP is not prone to a lysosomal degradation as endosomes do not fuse with lysosomes [51]. Accordingly, we did not observe any decrease of the fluorescence in the two cell lines in a suitable time after peptide exposure due to the release of peptide fragments outside the cells [52]. Heparin showed to be a less effective inhibitor. Indeed heparin has been used to decrease the binding of polyarginine CPPs to cell surfaces [53] and GAGs sequestering cationic peptides, may affect their biological effect [54]. The reason of a lower effect of heparin on proline-rich peptide internalization could be partially explained by the poor binding capacity of heparin to the two peptides as shown by size exclusion chromatography experiments where the elution volume of either p1932 or R.I.-p1932 did not significantly change upon interaction with increasing amounts of heparin. Although this aspect should be investigated in more detail, the poor binding may be explained with a fast equilibrium, and so a weak interaction, occurring between proline-rich peptides and heparin [55].

Endocytosis and hence peptide internalization are dependent on cell-cycle events [56]. Fielding and Royle have recently reported that mitosis completely inhibited the CDE pathway [57]. Interestingly, when mitosis was blocked by growing cells in a serum-free medium, the uptake was greatly reduced if compared to not synchronized (replicating) cells. These findings are in agreement with the inhibitor experiment data and enforce our hypothesis for a clathrin-independent endocytosis pathway at the basis of the proline-rich peptide uptake and further suggest that a dynamic rearrangement of the plasma membrane and of the cytoskeleton is determinant for peptide internalization.

Some authors have highlighted how the endocytosis pathway may differ depending on peptide characteristics and the cell type and different pathways have been proposed for cell-penetrating peptide internalization, evidencing a complex framework. Moreover, the same peptide may follows diverse pathways in the same cell type depending on different factors such as peptide concentration, structure and furthermore on cell physiological conditions [28,45,48,58]. For example, one of the critical factors which may affect the uptake pathway is the concentration of the peptide used. At higher concentrations a perturbation or even a disruption of the membrane may occur, leading to a passive entry of the peptide [59]. At the peptide concentrations employed in this study (10 and 20 μM), that however are near to those found in the oral cavity in saliva, we could not detect any membrane damage as evidenced by the microscopy observations, cytotoxicity, and artificial vesicle assays, performed even at concentrations well above those used in the uptake studies. We also tried to maintain when possible, a constant peptide to cell ratio, another critical point outlined in various CPP studies [60].

It is noteworthy that the two peptides follow an apparent similar endocytosis pathway independently on the cell type even if at different uptake rates. On the other side, the cytosolic distribution varies depending on the peptide form and the cell type. While the natural peptide largely diffuses in the cytosol and in the nuclei of PJ15 cells, the R.I. form is more confined in the same cells in vesicles and is less present in the nuclei. In hGFs both the peptides are completely absent in the nuclei.

These data suggest that nuclear receptors recognizing the proline-rich peptides, may be expressed in PJ15 cells and not, or in a lesser extent, in hGFs thus explaining the complete absence of peptide inside the nuclei of these cells[56]. This aspect is intriguing under an applicative point of view, as these proline-rich peptides may be successfully used as specific drug cargoes targeting such tumoral cells.

Although it is beyond the purpose of this study, these results let us to speculate about the physiological significance of p1932 peptide. Its ability to be internalized within the oral mucosa may allow this peptide to play potential intracellular functions. This may be intriguing as many cellular mechanisms are mediated by the interaction of proline stretches in certain proteins and the Proline-Rich Sequence (PRS) Recognition Domains, which include the SH3, GYF, EVH-1, profilin-like, and WW domains [61]. The proline-rich peptide PR39 is a clear example as a modulator of intracellular signals involving SH3 domains [7]. Cell proteomes are particularly rich in SH3 domains able to recognize the PxxP consensus sequences, and basic residues flanking this sequence may improve the recognition as well [62]. p1932 possesses these features and thus it represents a good candidate as an interactor of PRS domains and hence as a modulator of cell functions.

5. Conclusions

We showed that a salivary proline-rich peptide and its isomeric synthetic form were internalized within normal and tumoral oral mucosa cell lines. It should be considered that the oral cavity epithelium is continuously renewed by an exfoliation process, but the internalization time rates shown by p1932, allow the entry of the peptide in a suitable time to exert some biological role in the mouth mucosa. In our opinion the intracellular uptake of p1932 is of great interest in the oral biology, in fact, the entry within cells of the oral mucosa strongly suggests an intracellular physiological role of this peptide. These findings open a scenario in which p1932 and many peptides similar to it may play some roles as modulator molecules of cell machinery of oral epithelium.

In addition, the L- and retro-inverso proline-rich peptides possess a series of features that make them potential candidates for applications as nano-delivery systems. Both peptides offer practical advantages including good solubility in water, simplicity of synthesis, resistance to proteolytic degradation and hence a major bioavailability coupled with a low cytotoxicity for the D-retro form [41] and, in the case of p1932, a human origin. Compared to other CPPs, like penetratin used in this study as a positive control, these peptides represent at least a good starting point for the design of new biocompatible and efficient CPPs.

Conflict of interest

Giorgia Radicioni, Annarita Stringaro, Agnese Molinari, Giuseppina Nocca, Renato Longhi, Davide Pirolli, Emanuele Scarano, Federica Iavarone, Barbara Manconi, Tiziana Cabras, Irene Messana, Massimo Castagnola and Alberto Vitali.

All the authors have declared that no conflict of interests exists.

Acknowledgments

The authors acknowledge the financial support of Nando Peretti Foundation contract n° 2011/28, Catholic University of Rome D1 line 2012/13, Cagliari University CAR 2012/13, MIUR and Regione Sardegna 2012, CRP-60281 according to their programs of scientific diffusion. FAREBIO CNR project is also gratefully acknowledged.

References

[1] A. Vitali, Proline-rich peptides: multifunctional bioactive molecules as new potential therapeutic drugs, Curr. Protein Pept. Sci. 16 (2011) 147–162.
[2] W.P. Vermeij, B.I. Florea, S. Isenia, A. Alia, J. Brouwer, C. Backendorf, Proteomic identification of in vivo interactors reveals novel function of skin cornification proteins, J. Proteome Res. 11 (2012) 3068–3076.
[3] K.Y. Fung, C. Morris, S. Sathe, R. Sack, M.W. Duncan, Characterization of the in vivo forms of lacrimal-specific proline-rich proteins in human tear fluid, Proteomics 4 (2004) 3953–3959.
[4] A. Bacsi, M. Woodberry, M.L. Kruzel, I. Boldogh, Colostrinin delays the onset of proliferative senescence of diploid murine fibroblast cells, Neuropeptides 41 (2007) 93–101.
[5] T.K. Davtyan, H.M. Manukyan, G.S. Hakopyan, N.R. Mkrtchyan, S.A. Avetisyan, A.A. Galoyan, Hypothalamic proline-rich polypeptide is an oxidative burst regulator, Neurochem. Res. 30 (2005) 297–309.
[6] L. Otvos Jr., The short proline-rich antibacterial peptide family, Cell. Mol. Life Sci. 59 (2002) 1138–1150.
[7] Y.R. Chan, R.L. Gallo, PR-39, a syndecan-inducing antimicrobial peptide, binds and affects p130Cas, J. Biol. Chem. 44 (1998) 28978–28985.
[8] A. Migliaccio, G. Castoria, A. de Falco, A. Bilancio, P. Giovannelli, M. Di Donato, I. Marino, H. Yamaguchi, E. Appella, F. Auricchio, Polyproline and Tat transduction

peptides in the study of the rapid actions of steroid receptors, Steroids 77 (2012) 974–978.
[9] S. Conti, G. Radicioni, T. Ciociola, R. Longhi, L. Polonelli, R. Gatti, T. Cabras, I. Messana, M. Castagnola, A. Vitali, Structural and functional studies on a proline-rich peptide isolated from swine saliva endowed with antifungal activity towards *Cryptococcus neoformans*, Biochim. Biophys. Acta 1828 (2013) 1066–1074.
[10] M. Scocchi, A. Tossi, R. Gennaro, Proline-rich antimicrobial peptides: converging to a non-lytic mechanism of action, Cell. Mol. Life Sci. 68 (2011) 2317–2330.
[11] M. Mardirossian, R. Grzela, C. Giglione, T. Meinnel, R. Gennaro, P. Mergaert, M. Scocchi, The host antimicrobial peptide Bac71-35 binds to bacterial ribosomal proteins and inhibits protein synthesis, Chem. Biol. 21 (2014) 1639–1647.
[12] S. Pujals, E. Giralt, Proline-rich, amphipathic cell-penetrating peptides, Adv. Drug Deliv. Rev. 60 (2008) 473–484.
[13] S. Pujals, N.G. Bastffls, E. Pereiro, C. Lopez-Iglesias, V.F. Puntes, M.J. Kogan, E. Giralt, Shuttling gold nanoparticles into tumoral cells with an amphipathic proline-rich peptide, Chembiochem 6 (2009) 1025–1031.
[14] N.Q. Shi, W. Gao, B. Xiang, X.R. Qi, Enhancing cellular uptake of activable cell-penetrating peptide–doxorubicin conjugate by enzymatic cleavage, 7 (2012) 1613–1621.
[15] F.M. Amado, R.P. Ferreira, R. Vitorino, One decade of salivary proteomics: current approaches and outstanding challenges, Clin. Biochem. 46 (2013) 506–517.
[16] E.J. Helmerhorst, X. Sun, E. Salih, F.G. Oppenheim, Identification of Lys-Pro-Gln as a novel cleavage site specificity of saliva-associated proteases, J. Biol. Chem. 283 (2008) 19957–19966.
[17] M. Hardt, L.R. Thomas, S.E. Dixon, G. Newport, N. Agabian, A. Prakobphol, S.C. Hall, H.E. Witkowska, S.J. Fisher, Toward defining the human parotid gland salivary proteome and peptidome: identification and characterization using 2D SDS-PAGE, ultrafiltration, HPLC, and mass spectrometry, Biochemistry 44 (2005) 2885–2899.
[18] F.M. Amado, M.J. Lobo, P. Domingues, J.A. Duarte, R. Vitorino, Salivary peptidomics, Expert Rev. Proteomics 5 (2010) 709–721.
[19] I. Messana, T. Cabras, E. Pisano, M.T. Sanna, A. Olianas, B. Manconi, M. Pellegrini, et al., Trafficking and post-secretory events responsible for the formation of secreted human salivary peptides: a proteomics approach, Mol. Cell. Proteomics 5 (2008) 911–926.
[20] G.B. Fields, R.L. Noble, Solid phase peptide synthesis utilizing 0-fluorenylmethoxycarbonyl amino acids, Int. J. Pept. Protein Res. 35 (1990) 161–214.
[21] D. Quaglino, F. Boraldi, D. Barbieri, A. Croce, R. Tiozzo, I. Pasquali Ronchetti, Abnormal phenotype of in vitro dermal fibroblasts from patients with pseudoxanthoma elasticum (PXE), Biochim. Biophys. Acta 1501 (2000) 51–62.
[22] R. Tiozzo, R. Costa, M. Baccarani Contri, M.R. Cingi, I. Pasquali Ronchetti, R. Salvini, S. Rindi, G. De Luca, Pseudoxanthoma elasticum (PXE): ultrastructural and biochemical study on proteoglycan and proteoglycan-associated material produced by skin fibroblasts in vitro, Coll. Relat. Res. 8 (1988) 49–64.
[23] G. Nocca, R. Ragno, V. Carbone, G.E. Martorana, D.V. Rossetti, G. Gambarini, B. Giardina, A. Lupi, Identification of glutathione-methacrylates adducts in gingival fibroblasts and erythrocytes by HPLC-MS and capillary electrophoresis, Dent. Mater. 27 (2011) 87–98.
[24] R. Scotti, R. Tiozzo, C. Parisi, M.A. Croce, P. Baldissara, Biocompatibility of various root canal filling materials ex vivo, Int. Endod. J. 41 (2008) 651–657.
[25] E. Borenfreund, O. Borrero, In vitro cytotoxicity assays. Potential alternatives to the Draize ocular allergy test, Cell Biol. Toxicol. 1 (1984) 55–65.
[26] S. Kolusheva, T. Shahal, R. Jelinek, Peptide–membrane interactions studied by a new phospholipid/polydiacetylene colorimetric vesicle assay, Biochemistry 39 (2000) 15851–15859.
[27] J. Hed, G. Hallden, S.G. Johansson, P. Larsson, The use of fluorescence quenching in flow cytofluorometry to measure the attachment and ingestion phases in phagocytosis in peripheral blood without prior cell separation, J. Immunol. Methods 101 (1987) 119–125.
[28] J.P. Richard, K. Melikov, H. Brooks, P. Prevot, B. Lebleu, L.V. Chernomordik, Cellular uptake of unconjugated TAT peptide involves clathrin-dependent endocytosis and heparan sulfate receptors, J. Biol. Chem. 280 (2005) 15300–15306.
[29] C. Bechara, S. Sagan, Cell-penetrating peptides: 20 years later, where do we stand? FEBS Lett. 587 (2013) 1693–1702.
[30] H. Xia, X. Gao, G. Gu, Z. Liu, Q. Hu, Y. Tu, et al., Penetratin-functionalized PEG-PLA nanoparticles for brain drug delivery, Int. J. Pharm. 436 (2012) 840–850.
[31] M. Lukanowska, J. Howl, S. Jones, Bioportides: bioactive cell-penetrating peptides that modulate cellular dynamics, Biotechnol. J. 8 (2013) 918–930.
[32] W.C. Wimley, S.H. White, Experimentally determined hydrophobicity scale for proteins at membrane interfaces, Nat. Struct. Biol. 3 (1996) 842–848.
[33] M.J. Oudhoff, M.E. Blaauboer, K. Nazmi, N. Scheres, J.G. Bolscher, E.C. Veerman, The role of salivary histatin and the human cathelicidin LL-37 in wound healing and innate immunity, Biol. Chem. 391 (2010) 541–548.
[34] S. Tati, W.S. Jang, R. Li, R. Kumar, S. Puri, M. Edgerton, Histatin 5 resistance of *Candida glabrata* can be reversed by insertion of *Candida albicans* polyamine transporter-encoding genes DUR3 and DUR31, PLoS One 8 (4) (2013), e61480.
[35] M. Hans, V. Madaan. Epithelial antimicrobial peptides: guardian of the oral cavity. Int. J. Pept. 2014;2014:370297. doi: http://dx.doi.org/10.1155/2014/370297.
[36] P. de Sousa-Pereira, F. Amado, J. Abrantes, R. Ferreira, P.J. Esteves, R. Vitorino, An evolutionary perspective of mammal salivary peptide families: cystatins, histatins, statherin and PRPs, Arch. Oral Biol. 58 (2013) 451–458.
[37] F. Canon, F. Paté, V. Cheynier, P. Sarni-Manchado, A. Giuliani, J. Pérez, D. Durand, J. Li, B. Cabane, Aggregation of the salivary proline-rich protein IB5 in the presence of the tannin EgCG, Langmuir 29 (2013) 1926–1937.
[38] A. Berndt, P. Hyckel, A. Könneker, D. Katenkamp, H. Kosmehl, Oral squamous cell carcinoma invasion is associated with a laminin-5 matrix re-organization but independent of basement membrane and hemidesmosome formation. Clues from an in vitro invasion model, Invasion Metastasis 17 (1997) 251–258.
[39] S. Aubry, B. Aussedat, D. Delaroche, C.Y. Jiao, G. Bolbach, S. Lavielle, G. Chassaing, S. Sagan, F. Burlina, MALDI-TOF mass spectrometry: a powerful tool to study the internalization of cell-penetrating peptides, Biochim. Biophys. Acta 1798 (2010) 2182–2189.
[40] W.P. Verdurmen, P.H. Bovee-Geurts, P. Wadhwani, A.S. Ulrich, M. Hällbrink, T.H. van Kuppevelt, R. Brock, Preferential uptake of L- versus D-amino acid cell-penetrating peptides in a cell type-dependent manner, Chem. Biol. 18 (2011) 1000–1110.
[41] T. Holm, H. Räägel, S.E. Andaloussi, M. Hein, M. Mäe, M. Pooga, Ü. Langel, Retro-inversion of certain cell-penetrating peptides causes severe cellular toxicity, Biochim. Biophys. Acta 1808 (2011) 1544–1551.
[42] S. Soufian, H. Naderi-Manesh, A. Alizadeh, M. Nabi Sarbolouki, World Acad. Sci.Eng. Technol. 3 (2009) 742–748.
[43] M.C. Petit, N. Benkirane, G. Guichard, A.P. Du, M. Marraud, M.T. Cung, J.P. Briand, S. Muller, Solution structure of a retro-inverso peptide analogue mimicking the foot-and-mouth disease virus major antigenic site. Structural basis for its antigenic cross-reactivity with the parent peptide, J. Biol. Chem. 274 (1999) 3686–3692.
[44] E. Eiríksdóttir, K. Konate, U. Langel, G. Divita, S. Deshayes, Secondary structure of cell-penetrating peptides controls membrane interaction and insertion, Biochim. Biophys. Acta 1798 (2010) 1119–1128.
[45] F. Madani, S. Lindberg, U. Langel, S. Futaki, A. Graslund, Mechanisms of cellular uptake of cell-penetrating peptides, J. Biophys. 414729 (2011), http://dx.doi.org/10.1155/2011/414729.
[46] F. Duchart, M. Fotin-Mleczek, H. Schwarz, R. Fischer, R. Brock, A comprehensive model for the cellular uptake of cationic cell-penetrating peptides, Traffic 8 (2007) 848–866.
[47] I. Nakase, A. Tadokoro, N. Kawabata, T. Takeuchi, H. Katoh, K. Hiramoto, et al., Interaction of arginine-rich peptides with membrane-associated proteoglycans is crucial for induction of actin organization and macropinocytosis, Biochemistry 46 (2007) 492–501.
[48] D. Vercauteren, R.E. Vandenbroucke, A.T. Jones, J. Rejman, J. Demeester, S.C. De Smedt, N.N. Sanders, K. Braeckmans, The use of inhibitors to study endocytic pathways of gene carriers: optimization and pitfalls, Mol. Therapy 18 (2010) 561–569.
[49] R.G. Parton, A.A. Richards, Lipid rafts and caveolae as portals for endocytosis: new insights and common mechanisms, Traffic 4 (2003) 724–738.
[50] S. Pujals, J. Fernandez-Carneado, D. Ludevid, E. Giralt, D-SAP: a new, non-cytotoxic and fully protease resistant cell-penetrating peptide, ChemMedChem 3 (2008) 296–301.
[51] L. Pelkmans, A. Helenius, Endocytosis via caveolae, Traffic 3 (2002) 311–320.
[52] R. Fischer, K. Kohler, M. Fotin-Mleczek, R. Brock, A stepwise dissection of the intracellular fate of cationic cell-penetrating peptides, J. Biol. Chem. 279 (2004) 12625–12635.
[53] S. Al-Taei, N.A. Penning, J.C. Simpson, S. Futaki, T. Takeuchi, I. Nakase, A.T. Jones, Intracellular traffic and fate of protein transduction domains HIV-1 TAT peptide and octaarginine. Implications for their utilization as drug delivery vectors, Bioconjug. Chem. 17 (2006) 90–100.
[54] W. Barańska-Rybak, A. Sonesson, R. Nowicki, A. Schmidtchen, Glycosaminoglycans inhibit the antibacterial activity of LL-37 in biological fluids, J. Antimicrob. Chemother. 57 (2006) 260–265.
[55] C. Foerg, U. Ziegler, J. Fernandez-Carneado, E. Giralt, R. Rennert, A.G. Beck-Sickinger, H.P. Merkle, Decoding the entry of two novel cell penetrating peptides in Hela cells: lipid raft-mediated endocytosis and endosomal escape, Biochemistry 44 (2005) 72–81.
[56] G. Rádis-Baptista, B.G. de la Torre, D. Andreu, Insights into the uptake mechanism of NrTP, a cell-penetrating peptide preferentially targeting the nucleolus of tumour cells, Chem. Biol. Drug Des. 79 (2012) 907–915.
[57] A.B. Fielding, S.J. Royle, Mitotic inhibition of clathrin-mediated endocytosis, Cell. Mol. Life Sci. (2013), http://dx.doi.org/10.1007/s00018-012-1250-8.
[58] J. Mueller, I. Kretzschmar, R. Volkmer, P. Boisguerin, Comparison of cellular uptake using 22 CPPs in 4 different cell lines, Bioconjug. Chem. 19 (2008) 2363–2374.
[59] S.M. Fuchs, R.T. Raines, Pathway for polyarginine entry into mammalian cells, Biochemistry 43 (2004) 2438–2444.
[60] M. Hallbrink, J. Oehlke, G. Papsdorf, M. Bienert, Uptake of cell-penetrating peptides is dependent on peptide-to-cell ratio rather than on peptide concentration, Biochim. Biophys. Acta 1667 (2004) 222–228.
[61] L.J. Ball, R. Kuhne, J. Schneider-Mergener, H. Oschkinat, Recognition of proline-rich motifs by protein–protein-interaction domains, Angew. Chem. Int. Ed. 44 (2005) 2852–2869.
[62] A. Musacchio, How SH3 domains recognize proline, Adv. Protein Chem. 61 (2003) 211–255.